Industrial Crops & Products 122 (2018) 596–608

Contents lists available at ScienceDirect

Industrial Crops & Products

journal homepage: www.elsevier.com/locate/indcrop

Extraction, purification, and bioactivities analyses of polysaccharides from *Glycyrrhiza uralensis*

Yonggang Wang[a,*,1], Yuanli Li[a,1], Xueqing Ma[b], Haiwei Ren[a], Wenguang Fan[a], Feifan Leng[a,*], Mingjun Yang[a], Xiaoli Wang[c]

[a] School of Life Science and Engineering, Lanzhou University of Technology, Lanzhou, Gansu, 730050, PR China
[b] State Key Laboratory of Veterinary Etiological Biology, National Foot and Mouth Disease Reference Laboratory, Lanzhou Veterinary Research Institute, Chinese Academy of Agricultural Sciences, No.1 Xujiaping, Lanzhou 730046, Gansu, China
[c] Lanzhou Institute of Husbandry and Pharmaceutical Science of CAAS, Lanzhou, Gansu,730050, PR China

ARTICLE INFO

Keywords:
Polysaccharides
Optimization
Characterization
Antioxidant activity

ABSTRACT

Glycyrrhiza uralensis is an important traditional Chinese herbal medicine. Polysaccharide is one of active components of *G. uralensis*. In this paper, the extraction conditions of crude polysaccharides from *G. uralensis* (GPs0) were optimized by central composite design (CCD), and Three purified polysaccharide fractions (GPs1, GPs2 and GPs3) were studied based on physicochemical property, monosaccharide composition, molecular weight, structures characteristics and antioxidant activities. Results showed that the yield of GPs0 reached at the maximum of 4.23%, when the optimum extraction process was 1:13 g/mL (solid-liquid ratio), 600 W (ultrasonic power) at 70°C for 85 min. Except for GPs2, the others (GPs0, GPs1 and GPs3) are non-reducing sugars. They don't contain starch. GPs0 and GPs1 contain protein. The molecular weight, monosaccharide composition and Fourier transform infrared spectroscopy (FT-IR) assay showed that GPs1, GPs2 and GPs3 are pyran polysaccharides with a weight average molecular weight (Mw) of 4.513×10^3, 1.378×10^5 and 2.084×10^5 g/mol, respectively. GPs1, GPs2 and GPs3 mainly contain glucose and galactose, respectively. Scanning electron microscope (SEM) demonstrated that GPs1, GPs2 and GPs3 are flaky with a pore structure. Atomic force microscopy (AFM) displayed GPs1 and GPs2 have a large number of dispersions and a small amount of smaller globular aggregates, while GPs3 is the opposite of the abovementioned result. Besides, the antioxidant activity assay of these polysaccharides illustrated that GPs1 has a strong scavenging effect on DPPH radicals and superoxide radical.

1. Introduction

Glycyrrhiza uralensis (*G. uralensis*) named 'Gancao', belongs to the Leguminosae family, which has been known as a traditional Chinese medicine to treat various diseases such as respiratory ailments, inflammatory disorders, heartburn, gastritis, liver problems and skin diseases (Cheng et al., 2008; Zhang et al., 2015). Many studies have indicated that the major bioactive ingredients of *G. uralensis* include flavonoids, polysaccharides and triterpene saponins (Prabhjit et al., 2012) Since 1969, *Lentinus edodes* polysaccharide with a good anti-tumor activity was first discovered by Chihara in Japan (Chihara et al., 1969), the studies of polysaccharides have been paid more and more attention on the extraction, purification and bioactivity determination. Polysaccharides formed by a number of monosaccharides (Li and Shah, 2014) have many physiological activities such as strengthening immunity, anti-tumor, and antiviral (Rui et al., 2016; Yi et al., 2017), and have been applied to drugs, agriculture, health-food market, cosmetics (Patel et al., 2013) and biological materials. In our pervious studies, we have reported that herbal polysaccharide mixed with hydroxyapatite (HAp), polylactic acid (PLA) or squid skin collagen as biological material could be applied in the tissue engineering (Zhang et al., 2013, 2016; Zhang et al., 2017), and also more and more studies showed gelatin with the good cross linking feature could mix with polysaccharide or metal ions (Zinatloo-Ajabshir and Salavati-Niasari, 2015, Zinatloo-Ajabshir and Salavati-Niasari, 2016a,b; Zinatloo-Ajabshir and Salavati-Niasari, 2017, Zinatloo-Ajabshir et al., 2016a,b; Zinatlooajabshir et al., 2018a,b), which provide a novel idea to prepare nanoparticles biomaterial in drugs (Qazvini and Zinatloo, 2011; Zinatloo and Qazvini, 2014, 2015).

Until now, the polysaccharides from *G. uralensis* (GPs) have been

* Corresponding authors at: School of Life Science and Engineering, Lanzhou University of Technology, Langongping Road 287, Qilihe District, Lanzhou, Gansu, PR China.
E-mail addresses: 412316788@163.com (Y. Wang), lff0928@sina.com (F. Leng).
[1] Co-first author.

https://doi.org/10.1016/j.indcrop.2018.06.011
Received 22 November 2017; Received in revised form 31 May 2018; Accepted 4 June 2018
Available online 17 June 2018

reported to have antitumor, anti-inflammatory, antiviral, immunomodulatory, antioxidant and antimicrobial activities (Chen et al., 2016, 2017; Jiang et al., 2016; Maclennan et al., 2016). Yi et al. (2017) discovered that the immune-modulating activity of *glycyrrhiza polysaccharide* can be improved significantly by encapsulated with liposome.

Different extraction methods and source of *G. uralensis* will affect the extraction rate, physicochemical properties, structure and bioactivity of polysaccharide significantly. More and more extraction techniques such as aqueous extraction, pressurized water extraction (PWE), ultrasonic-assisted extraction (UAE), and microwave-assisted extraction (MAE) (Feng et al., 2015; Yuan and Macquarrie, 2015) were used to extract polysaccharides. UAE is the most useful method to replace conventional extraction techniques for extraction of polysaccharides,combined with the optimal statistical experimental designs (Shen et al., 2014). Response surface methodology (RSM) is a collection of statistical techniques, including experiment designing, model building, evaluation of factors, and searching for optimal conditional factors (Ghasemzadeh et al., 2015), which has been used for optimizing extraction conditions for extraction of polysaccharides (Aguiló-Aguayo et al., 2017; Ji et al., 2017; Ma et al., 2016; Ren et al., 2017; Romdhane et al., 2017; Yang et al., 2017). Until now, there have been some reports on the extraction, isolation and characteristic analysis of polysaccharide from *G. uralensis*. Polysaccharide of *G. uralensis* from Yanchi, Ningxia, China was extracted by hot water reflux (HWE) with the given condition of hot water (1:9, w/v) at 80 ℃ for 1 h, and then purified to obtain three water-soluble polysaccharides fractions (GUPs-1, GUPs-2 and GUPs-3) for the analysis of physicochemical properties and antioxidant activities (Zhang et al., 2015). Meanwhile, the hot water reflux extraction of polysaccharide of *G. uralensis* from Shihezi, Xinjiang, China with was optimized by response surface methodology, and the purified product (GUP-II) possesses excellent antioxidant and immunological activities (Chen et al., 2017). According to the abovementioned research progress, we could find there are little published reports on the isolation, purification, composition, structure and activity of polysaccharide from Minxian, Gansu, China. Especially, the optimization of ultrasonic-assisted extraction polysaccharides from *G. uralensis* by RSM have not been reported. In this study, the processing parameters for UAE-assisted extraction of crude polysaccharides (GPs0) from *G. uralensis* were optimized by RSM, and physicochemical property, monosaccharide composition, molecular weight, structures characteristics and antioxidant properties of the purified fraction were determined by multiple spectroscopy techniques. The study could provide a foundation for illuminate the structure-activity relationships of different purified polysaccharides from *G. uralensis*.

2. Materials and methods

2.1. Extraction and determination of crude polysaccharides

G. uralensis purchased from De Sheng Tang Pharmacy, Minxian, Gansu Province, China, were smashed and passed through 40 mesh sieve. The powders were defatted using petroleum ether. The ultrasonic assisted extraction (UAE) was used to obtain GPs according to the central composite design (CCD), described by Ying et al. (2011) and Prakash et al. (2013). In detail, *G. uralensis* powder (100 g) mixed with an appropriate amount of distilled water in a 500 mL round bottomed flask was ultrasonic-assisted treated in an ultrasonic processor (KQ-250DB, Kunshan Ultrasonic Instruments Co., Ltd., Jiangsu, China). The extraction conditions such as solid-liquid ratio, extraction temperature, extraction duration, and ultrasonic power were fixed at 1:10-1:20 g/mL, 65–75 °C, 50–70 min and 400–600 W, respectively. The extracts were purified by removing lipids, proteins and other components with different organic solvents, respectively. Meanwhile, the supernatant was separated, concentrated in a vacuum concentrator, and precipitated with four times volumes of 90% (v/v) ethanol for 24 h at 4 °C, and the crude GPs0 was obtained by vacuum freeze drying (FD-1A-50, Boyikang Instruments Co., Ltd., Beijing, China).

Table 1
Design and Results of RSM.

No.	A (Extraction temperature, ℃)	B (Extraction duration, min)	C (Solid-liquid ratio, g/mL)	D (Ultrasonic power, W)	Y (Extraction yield, %)
1	1 (75)	1 (90)	1 (1:20)	−1 (400)	3.11
2	1 (75)	1 (90)	−1 (1:10)	−1 (400)	2.82
3	1 (75)	−1 (70)	1 (1:20)	1 (600)	3.42
4	−1 (65)	1 (90)	−1 (1:10)	1 (600)	3.36
5	1 (75)	−1 (70)	−1 (1:10)	1 (600)	3.24
6	−1 (65)	−1 (70)	1 (1:20)	−1 (400)	3.31
7	−1 (65)	1 (90)	1 (1:20)	1 (600)	3.76
8	−1 (65)	−1 (70)	−1 (1:10)	−1 (400)	3.21
9	−1 (65)	0 (80)	0 (1:15)	0 (500)	3.49
10	1 (75)	0 (80)	0 (1:15)	0 (500)	4.21
11	0 (70)	−1 (70)	0 (1:15)	0 (500)	4.02
12	0 (70)	1 (90)	0 (1:15)	0 (500)	4.19
13	0 (70)	0 (80)	−1 (1:10)	0 (500)	3.69
14	0 (70)	0 (80)	1 (1:20)	0 (500)	4.16
15	0 (70)	0 (80)	0 (1:15)	−1 (400)	3.89
16	0 (70)	0 (80)	0 (1:15)	1 (600)	4.24
17	0 (70)	0 (80)	0 (1:15)	0 (500)	4.26
18	0 (70)	0 (80)	0 (1:15)	0 (500)	4.19
19	0 (70)	0 (80)	0 (1:15)	0 (500)	4.21
20	0 (70)	0 (80)	0 (1:15)	0 (500)	4.24
21	0 (70)	0 (80)	0 (1:15)	0 (500)	4.27

The content of GPs0 was determined at 485 nm (OD485) by phenol-sulfuric method (Dubois et al., 1956), calculated with linear regression equation ($Y = 0.0607X - 0.0569$, $R^2 = 0.9977$), the linear range of glucose concentration is 0–50 μg/mL. The yield of GPs0 could be calculated as follows:

$$GPs0\,\text{yield}(\%) = \frac{C \times N \times V}{W \times 1000} \times 100\%$$

where C denotes the concentration of polysaccharides (mg/mL); N denotes the dilution factor; V denotes the volume of extraction solution (mL); W denotes the weight of raw materials (g).

2.2. Extraction optimization

Based on the results of single-factor experiments and design principle of the response surface center combination experiments, four independent variables (solid-liquid ratio, extraction temperature, ultrasonic power, extraction duration) were used to optimize the yield of GPs0 at three levels. The twenty-one experimental points in Table 1 represented the coded and non-coded values of the experimental variables. Five repetitions (17–21) were used to calculate the pure error. Experimental results exhibited that response variables were fitted by a quadratic polynomial model set, and its general form was as follows:

$$Y = \beta_0 + \sum_{i=1}^{4} \beta_i x_i + \sum_{i=1}^{4} \beta_{ii} x_i^2 + \sum \sum_{i<j=1}^{4} \beta_{ij} x_i x_j$$

where Y is the measured response associated with each factor lever combination; β_0, β_i, β_{ii} and β_{ij} are the regression coefficients for intercept, linear, quadratic and interaction terms, respectively; x_i and xj are the coded independent variables. DesignExpert Software (Version 8.0.5) was used to estimate the response of each experimental design and optimize conditions. The fitness of the quadratic polynomial model was inspected by the regression coefficient R^2. F-value and P-value

were used to check the significance of the regression coefficient.

2.3. Purification of GPs

According to the abovementioned method, the GPs0 was extracted, freeze-dried, re-dissolved in distilled water into a concentration of 20 mg/mL. 1 mL of the sample filtered through a DEAE-52 cellulose chromatography column (2.6 × 20 cm) was equilibrated with distilled water. The polysaccharides were fractionated and eluted with distilled water and various concentrations of NaCl solution (0, 0.1 and 1 mol/l NaCl). The eluate was collected at 1 mL/min flow rate and each test tube (3 mL) by an automated step-by-step fraction collector and monitored by the phenol-sulfuric acid method. The main fraction was further purified through Sephadex G-100 column (2.0 × 30 cm), dialyzed with the deionized water, and lyophilized for further research.

2.4. Physicochemical properties analyses of GPs

Phenol-sulfuric acid procedure (Dubois et al., 1956), iodination reaction (Lee et al., 1994), Fehling's test (F. Schneider, 1979), carbazole reaction (Bitter and Muir, 1962), ninhydrin reaction (Sarin et al., 1981) and barium chloride-gelatin method (Kawai et al., 1969) were applied to determine the physicochemical properties of GPs, respectively.

2.5. Molecular weight of GPs

The molecular weight of GPs were evaluated by high performance size exclusion chromatography (HPSEC, DAWN EOS, Wyatt Technology Co., USA) with online multi-angle light scattering (MALLS). MALLS measurements were carried out on a multi-angle laser photometer (MALLS, DAWN®, HELEOS, Wyatt Technology Co., Santa Barbara, CA, USA) at 690.0 nm coupled with an Ultrahydrogel™ column (7.8 × 300 mm, Waters, USA). An Optilab refractometer (Dawn®, Wyatt Technology Co., Santa Barbara, CA, USA) was simultaneously connected. The solvent was filtered through filter with 0.2 μm membrane filter and degassed using an ultrasonic cleaner (KQ-250DB, Kunshan Ultrasonic Instrument Co., Ltd., China). 50 μL GPs solution was injected and eluted with the flow rate of 0.5 mL/min. The collected data were analyzed using the Astra Software (Version 5.3.1). The specific refractive index increments (dn/dc) of the polysaccharides in distilled water was measured at 690 nm by Optilab refractometer at room temperature. The value of dn/dc was 0.135 mL/g.

2.6. Monosaccharide and FT-IR analysis

Gas chromatography and mass spectrometry (GC–MS, Agilent Technologies Inc., USA) was applied to determine the monosaccharide composition according to Huang et al. (2006). Fourier transform infrared spectroscopy (FT-IR, FTS3000, PE, Co., Ltd., USA) analysis of the sample was obtained by grinding the mixture of polysaccharides and dry KBr. Spectral scanning was performed in a range of 500-4000 cm^{-1} with a resolution of 4 cm^{-1} on a Fourier transform infrared spectrophotometer (Thermo Scientific Nicolet iN10). At least 10 scans were performed for all spectra.

2.7. Scanning electron microscope observation

The three purified polysaccharides (GPs1, GPs2 and GPs3) were gold-plated 160 s by coating apparatus with 10 Pa vacuum and ion current of 15 mA, then the surface morphology of GPs was observed by Scanning electron microscope (SEM, JSM-6701 F, Japan Electronic Optics Co, Japan) (Jun et al., 2010).

2.8. Atomic force microscope observation

GPs1, GPs2 and GPs3 were dissolved in distilled water to a stock solution of 0.1 mg/mL, which was stirred for 2 h at 70 °C for dissolve completely. The stock solution was then diluted into 0.1 μg/mL with distilled water or blended with sodium dodecyl sulfate (SDS) at a ratio of 1:1 (GPs:SDS, w/w). The diluted solutions were stirred for 6 h at 60 °C. 10 μL of sample were deposited on a cleaved mica for 10 min, rinsed with 1 mL distilled water, dried with air. Atomic force microscope (AFM, 5500, Agilent Technologies, USA) was used for the scanning of surface topologies in the dry state under tapping mode.

2.9. Determination of bioactivities of GPs in vitro

2.9.1. Hydroxyl radical scavenging assay

Hydroxyl radical scavenging activity was determined according to Jin et al. (1996) with appropriate modifications. Reaction mixtures including 0.5 mL of 5.0 mM salicylic acid solution, 0.5 mL of 7.5 mM $FeSO_4$ solution, 0.5 mL of 0.1% H_2O_2 solution, 0.5 mL of the polysaccharides solution with different concentration (0.25, 0.5, 0.75, 1.0, 1.5, 2.0, 2.5, 3.0, 3.5 and 4.0 mg/mL, respectively) and 3 mL distilled water, were incubated at 37 °C for 30 min, and the absorbance of which was determined at 510 nm. The scavenging activity of hydroxyl radical production was measured as follows:

$$\text{Scavenging activity}(\%) = (1 - \frac{A_1 - A_2}{A_0}) \times 100\%$$

where A_0 denotes the absorbance of the control group in the hydroxyl radical generation system (water instead of GPs solution), A_1 denotes the absorbance of the test group, and A_2 denotes the absorbance of the control (water instead of H_2O_2 solution), respectively.

2.9.2. Superoxide radical scavenging assay

Superoxide radical scavenging activity of GPs1, GPs2 and GPs3 were measured according to Yuan and Gao (1997) with necessary modifications. Firstly, the polysaccharides were diluted to different concentration (0.25, 0.5, 0.75, 1.0, 1.5, 2.0, 2.5, 3.0, 3.5 and 4.0 mg/mL). Secondly, GPs in Tris-HCl buffer (pH 8.2) were incubated at 25 °C for 20 min, and then pyrogallol were added into the mixture and kept at 25 °C for 4 min. The reaction was terminated by addition of 1 mL 10 M HCl. The absorbance of the mixture was determined at 325 nm, and 50 mM phosphate buffer (pH 7.2) was used as the control. The scavenging activity of superoxide radical was computed by the following formula:

$$\text{Scavenging activity}(\%) = \left(1 - {}^{A_1}\!/_{A_0}\right) \times 100\%$$

where A_0 represents the absorbency variation of the control in the surperoxide radical generation system and A_1 represents the absorbance change of the treatment group.

2.9.3. Effect of scavenging of (DPPH) radicals

The DPPH scavenging assay was based on the method of Shimada et al. (1992). The solution of 0.2 mM DPPH in 60% ethanol was prepared before UV measurements. Then, the solution including 2.0 mL of the polysaccharides and 2.0 mL DPPH was kept at room temperature for 30 min in the dark, the absorbance of which at 525 nm was measured. Ascorbic acid was used as the positive controls. The scavenging activity of DPPH radical (%) was calculated as follows:

$$\text{Scavenging activity}(\%) = (1 - \frac{A_i - A_j}{A_0}) \times 100\%$$

where A_0 denotes the absorbance of DPPH solution without sample; A_i denotes the absorbance of the test sample mixed with DPPH solution, and Aj denotes the absorbance of the sample without DPPH solution.

2.9.4. Total reduce power assay

The total reduce power assay was carried out according to Deng et al. (2011). The reaction mixture containing 1 mL of phosphate buffer

(pH 6.6, 0.2 M), 1 mL of potassium ferricyanide (1%, w/v), and PNEP solution was incubated at 50 °C for 20 min. The reaction was terminated by addition of 1 mL of trichloroacetic acid (10%, w/v) to the mixture. After addition of 4 mL deionized water and 1 mL of $FeCl_3$ solution (0.1%, w/v), the solution was incubated at room temperature for 10 min, the absorbance of which was measured at 700 nm. Ascorbic acid was used as the positive control.

2.10. Statistical analysis

All data were based on mean values of triplicate. The difference was deemed to be significant when $P < 0.05$. The Origin Pro Software Package 8.5 (Origin Lab. Corp.) and Design Expert Software Version 8.0.5 (Stat-Ease Inc.) were applied to the statistical analysis.

3. Results and discussions

3.1. Optimization of extraction conditions

3.1.1. Establishment of regression model and analysis of variance (ANOVA)

The values of yield of polysaccharides to different levels combinations of the variables were given in Table 1. Based on multiple regression analysis of the experimental data, the response variables and the test variables were related by the following second-order polynomial equation:

$$Y = -26.72 + 1.06A - 9.26 \times 10^{-3}B + 1.81 \times 10^{-2}C - 1.91 \times 10^{-3}D + 1.16 \times 10^{-4}AB - 1.0 \times 10^{-4}AC + 4.17 \times 10^{-5}AD + 1.025 \times 10^{-3}BC + 4.9125 \times 10^{-4}BD = 4.75 \times 10^{-5}CD - 7.72 \times 10^{-3}A^2 - 1.09 \times 10^{-3}B^2 - 8.57 \times 10^{-3}C^2 - 2.19 \times 10^{-5}D^2$$

Where Y is the polysaccharides yield; A, B, C, and D are extraction temperature, extraction duration, ratio of water to raw materials, ultrasonic power, respectively.

The value of the determination coefficient ($R^2 = 0.9969$) from the ANOVA of the quadratic regression model indicated that it is a high correlation between the observed and predicted value. The model could be used to optimize the conditions of the GPs0 extraction. The analysis of variance suggested that the independent variables (A, C and D), quadratic terms (A_2, C_2 and D_2) and interaction terms (BD) significantly affected the polysaccharides yield ($P < 0.01$, $F \approx 135.7391$) as shown in Table 2, which exhibited that the extraction temperature is the most significant factor influenced GPs0 yield followed by solid-liquid ratio, ultrasonic power and extraction duration.

3.1.2. Interaction analysis of regression model

The effect of various factors on the yield of GPs0 and the interaction among various factors were shown in Figs. 1and Figure 2. In order to assess the effects of the four parameters (extraction temperature, extraction duration, solid-liquid ratio and ultrasonic power) on the yield of GPs0, two variables within the experimental range were described in a 3D surface plots while the other two variables remained unchanged at zero level. As shown in Fig. 1, the response surface opening down indicates the response value increases with the increasing of each factor, and then decreases, which indicates the model is stable and the stationary point is a maximum. The shapes of the contour plots shown whether the interactions among variables were significant (Wang et al., 2015). Six independent response surface plots were shown in Figs. 1 and 2.

Figs. 1a and Figure 2a demonstrated the effects of extraction temperature (A) and extraction duration (B) on the yield of GPs0. The yield increased to stable by the increase of temperature gradually. Compared with extraction duration, the effect of extraction temperature was more significant, but the effect of their interaction was not significant. This result was consistent with Wang et al. (2015). The effects of extraction temperature (A) and solid-liquid ratio (C) on the yield of GPs0 was shown in Figs. 1b and Figure 2b, which indicated that extraction temperature could affect the yield obviously. The interaction between extraction temperature (A) and ultrasonic power (D) exhibited non-significant on the yield of GPs0 as shown in Figs. 1c and Figure 2c. The effects of extraction duration (B) and solid-liquid ratio (C) on the production of GPs0 significantly as displayed in Figs. 1d and Figure 2d. However, both ultrasonic power (D) and extraction duration (B) has a negative effect on the yield of GPs0, the yield decreased with the increase of ultrasonic power and extraction duration in Figs. 1e and Figure 2e. And the results in Figs. 1f and Figure 2f displayed the interaction between solid-liquid ratio (C) and ultrasonic power (D) also cannot significantly affect the yield of GPs0. Among the four extraction parameters, extraction temperature was the most important factor affecting the yield of GPs0, followed by solid-liquid ratio, ultrasonic power and extraction duration. The optimal extraction conditions of GPs0 were obtained as follows: 1:12.85 g/mL (solid-liquid ratio), 564.08 W (ultrasonic power), 69.45 °C (extraction temperature), and 85.53 min (extraction duration), a maximum yield predicted of the GPs0 was 4.40%.

Table 2
Analysis of variance for fitted quadratic polynomial model.

Source	SS	DF	MS	F-value	P-value	Significance
Model	4.519227	14	0.322802	135.7391	< 0.0001	**
A	0.2592	1	0.2592	108.9943	< 0.0001	**
B	0.00045	1	0.00045	0.189226	0.6788	
C	0.13225	1	0.13225	55.6115	0.0003	**
D	0.06125	1	0.06125	25.7558	0.0023	**
AB	0.000123	1	0.000123	0.051512	0.828	
AC	0.000113	1	0.000113	0.047307	0.835	
AD	0.001563	1	0.001563	0.657036	0.4486	
BC	0.021013	1	0.021013	8.835816	0.0249	*
BD	0.386123	1	0.386123	162.3656	< 0.0001	**
CD	0.004513	1	0.004513	1.897519	0.2175	
A^2	0.481366	1	0.481366	202.4158	< 0.0001	**
B^2	0.030462	1	0.030462	12.80921	0.0117	*
C^2	0.117168	1	0.117168	49.26937	0.0004	**
D^2	0.122701	1	0.122701	51.59599	0.0004	**
Residual	0.014269	6	0.002378			
Lack of fit	0.009749	2	0.004874	4.313553	0.1003	
Pure error	0.00452	4	0.00,113			
Cor. total	4.533495	20				

$R^2 = 0.9969$, $R^2_{Adj} = 0.9895$, "**" very significant ($P < 0.01$), "*" significant ($0.01 < P < 0.05$).
Note: SS denotes sum of squares; DF denotes degree of freedom; MS denotes mean square.

3.1.3. Validation of the models

Taking the error from the actual operation into consideration, the optimal extraction conditions was revised as follows: the samples with solid-liquid ratio of 1:13 g/mL were incubated at 70 °C under 600 W for 85 min A verification experiment was carried out to validate the adequacy of the model under the revised optimal conditions, the yields of GPs0 was (4.23 ± 0.01)%. Compared with the theoretical prediction value (4.40%), the relative error was about 3.86%, which demonstrated that the extraction parameters obtained by the model are accurate, reliable and practical.

3.2. Purification of polysaccharides and physicochemical property analysis

The GPs0 solution was separated and purified by anion exchange chromatography on a DEAE-52 cellulose column, three independent elution peaks were obtained by phenol-sulfuric acid assay (Fig. 3). The acidic polysaccharide GPs1, GPs2 and GPs3 were eluted with a higher salt concentration. The three fractions were collected, concentrated and

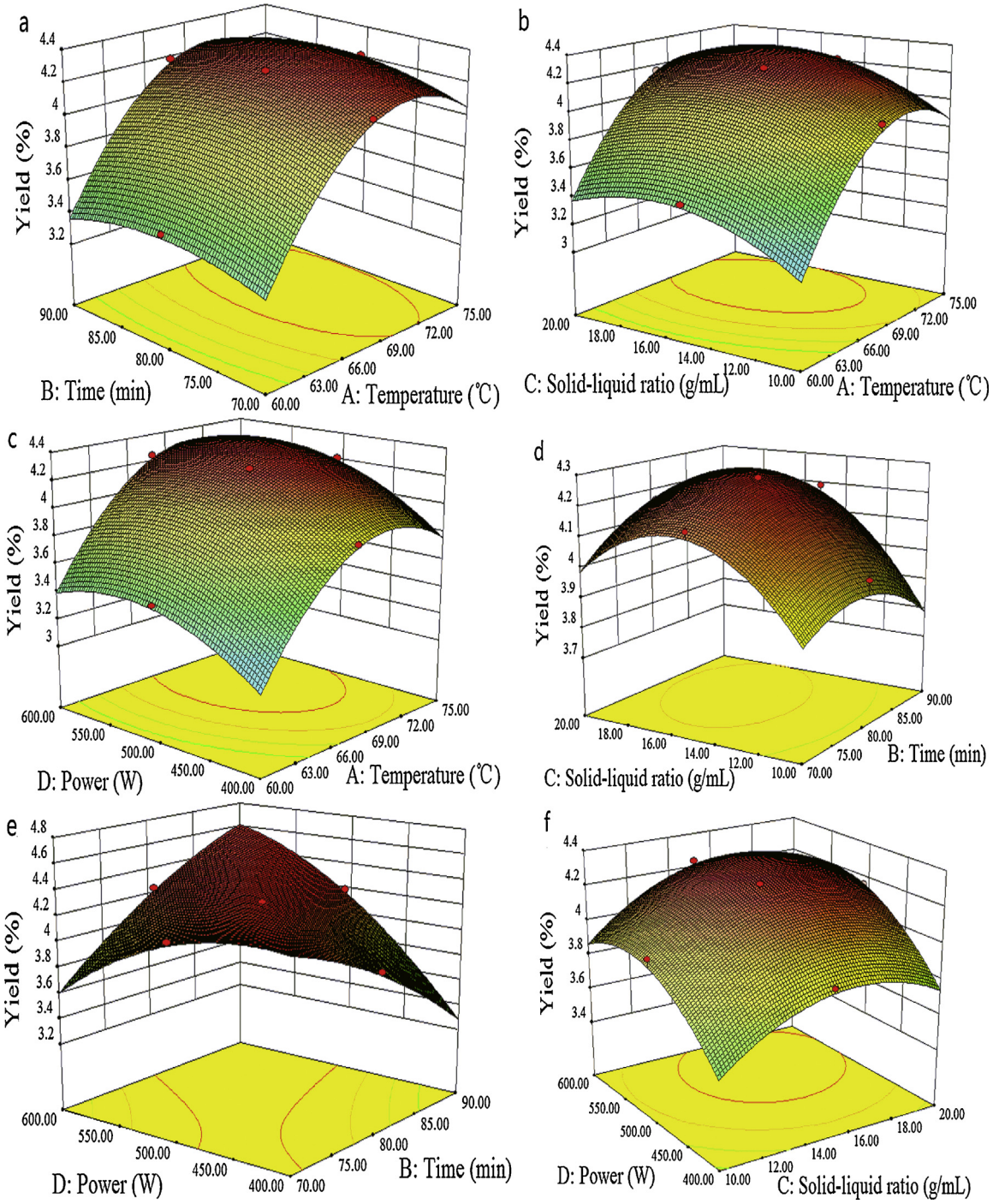

Fig. 1. Response surface plots for the mutual effects of (a) Temperature and time; (b) Temperature and solid-liquid ratio; (c) Temperature and power; (d) Time and solid-liquid ratio; (e) Time and power; (f) Solid-liquid ratio and power on the yield of GPs0.

purified by gel filtration chromatography with the Sephadex G-100. Three single elution peaks (GPs1, GPs2 and GPs3) were obtained, respectively. According to the Supplementary Table S1, crude polysaccharide from Yanchi, Ningxia, China extracted by hot water reflux was purified with the same method and three fractions (GUPs-1, GUPs-2 and GUPs-3) were obtained (Zhang et al., 2015). However, five fractions of crude GUP of *G. uralensis* from Shihezi, Xinjiang, China were obtained by the purified technology with DEAE cellulose-32 (Chen et al., 2017).

The analysis results of physicochemical properties of GPs0, GPs1, GPs2 and GPs3 indicated that except for GPs2, the others are non-reducing sugars. They don't contain starch, while GPs0 and GPs1 contain protein. The uronic acid contents of four polysaccharides were determined according to carbazole reaction. The uronic acid contents of GPs0 and GPs3 were 4.08% and 18.62%, respectively. No uronic acid existed in GPs1 and GPs2. The sulfate contents of four polysaccharides followed the order: GPs0 (3.85%), GPs2 (3.67%), GPs3 (3.42%) and GPs1 (1.58%), respectively. This result proved GPs0, GPs1, GPs2 and GPs3 are acidic polysaccharides. Many studies displayed the crude and purified polysaccharides of *G. uralensis* from different regions showed significant difference in the physicochemical properties by different extraction and purification technology as shown in Supplementary Table S1.

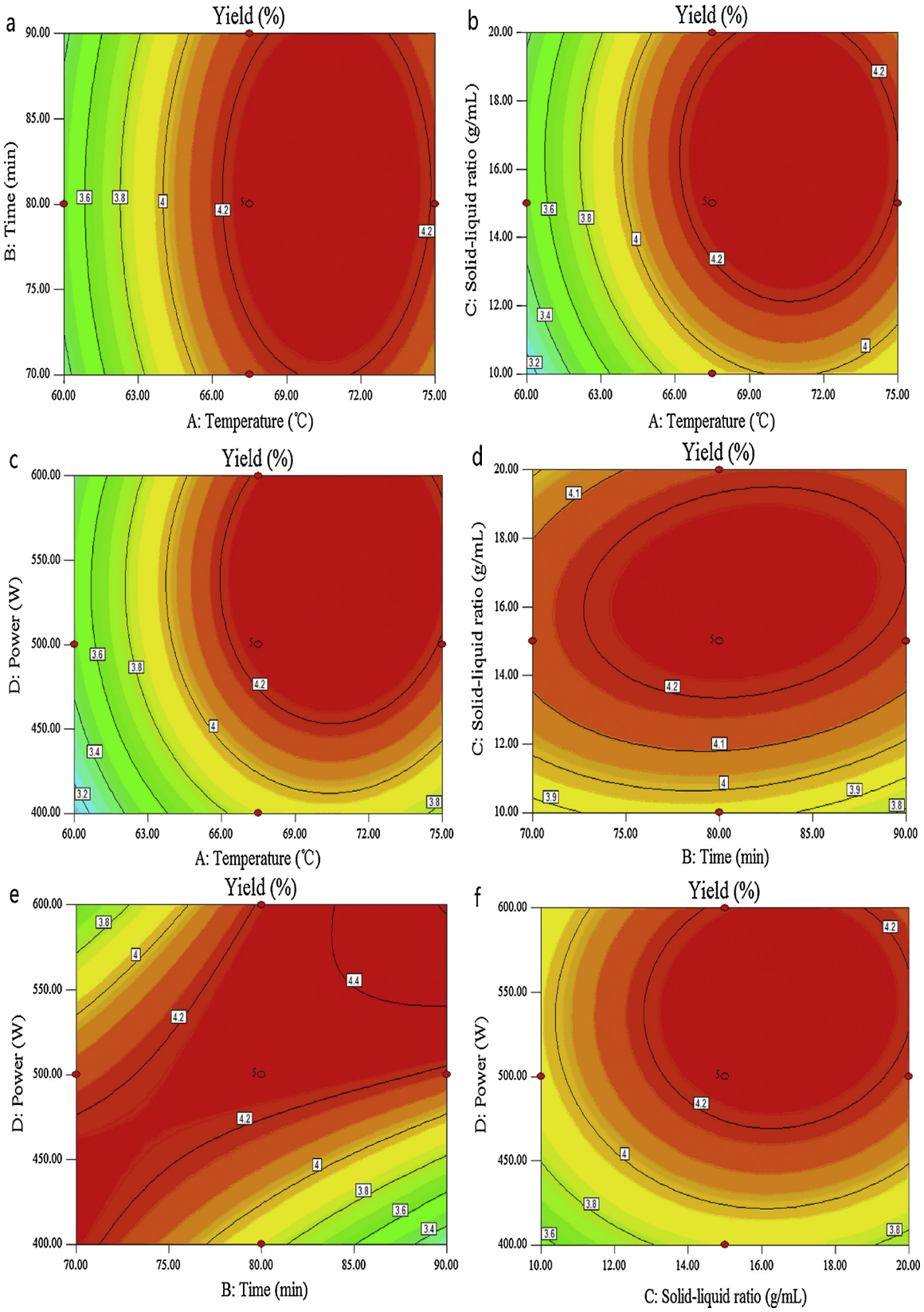

Fig. 2. Contour plots for the mutual effects of (a) Temperature and time; (b) Temperature and.
solid-liquid ratio; (c) Temperature and power; (d) Time and solid-liquid ratio; (e) Time and power; (f) Solid-liquid ratio and power on the yield of GPs0.

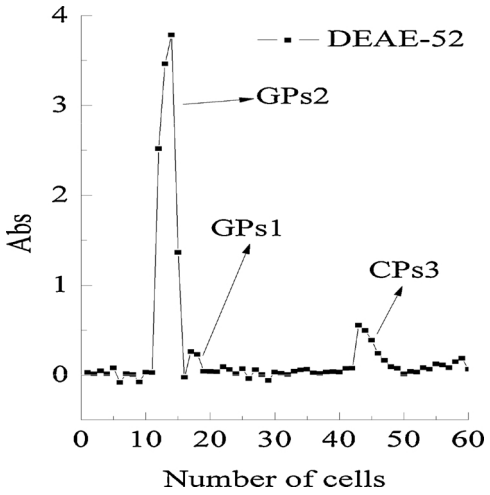

Fig. 3. Elution curve of GPs0 by DEAE-52 cellulose column.

3.3. Molecular weight

Natural polysaccharides have different chemical composition, molar mass and chain conformation, and have significant influence on their end-use of structure property relationship (Wang et al., 2010). The molecular weight and chain conformation of the purified GPs1, GPs2 and GPs3 determined by HPSEC-MALLS were shown in Fig. 4. The chromatograms of GPs1, GPs2 and GPs3 didn't exhibit a single peak, implying that there were aggregation and the inhomogeneity of the purified samples. The values of number-average molecular weight (Mn), weight average molecular weight (Mw), polydispersity indexes (PD, Mw/Mn) of three purified fractions (GPs1, GPs2 and GPs3) were

Table 3
Molecular characterization of three purified fractions (GPs1, GPs2 and GPs3) by HPSEC-MALLS.

Sample	Fractions	Mn	Mw	Mw/Mn
GPs1	Peak 1	1.267×10^3	4.513×10^3	3.561
	Peak 2	3.998×10^2	8.349×10^2	2.088
GPs2	Peak 1	1.077×10^5	1.378×10^5	1.279
	Peak 2	4.299×10^3	8.559×10^3	1.991
	Peak 3	2.696×10^2	2.871×10^2	1.065
GPs3	Peak 1	1.592×10^5	2.084×10^5	1.309
	Peak 2	3.554×10^3	1.092×10^4	3.073
	Peak 3	2.247×10^2	2.606×10^2	1.160

Note: Mn represents number-average molecular weight, Mw is weight-average molecular weight.

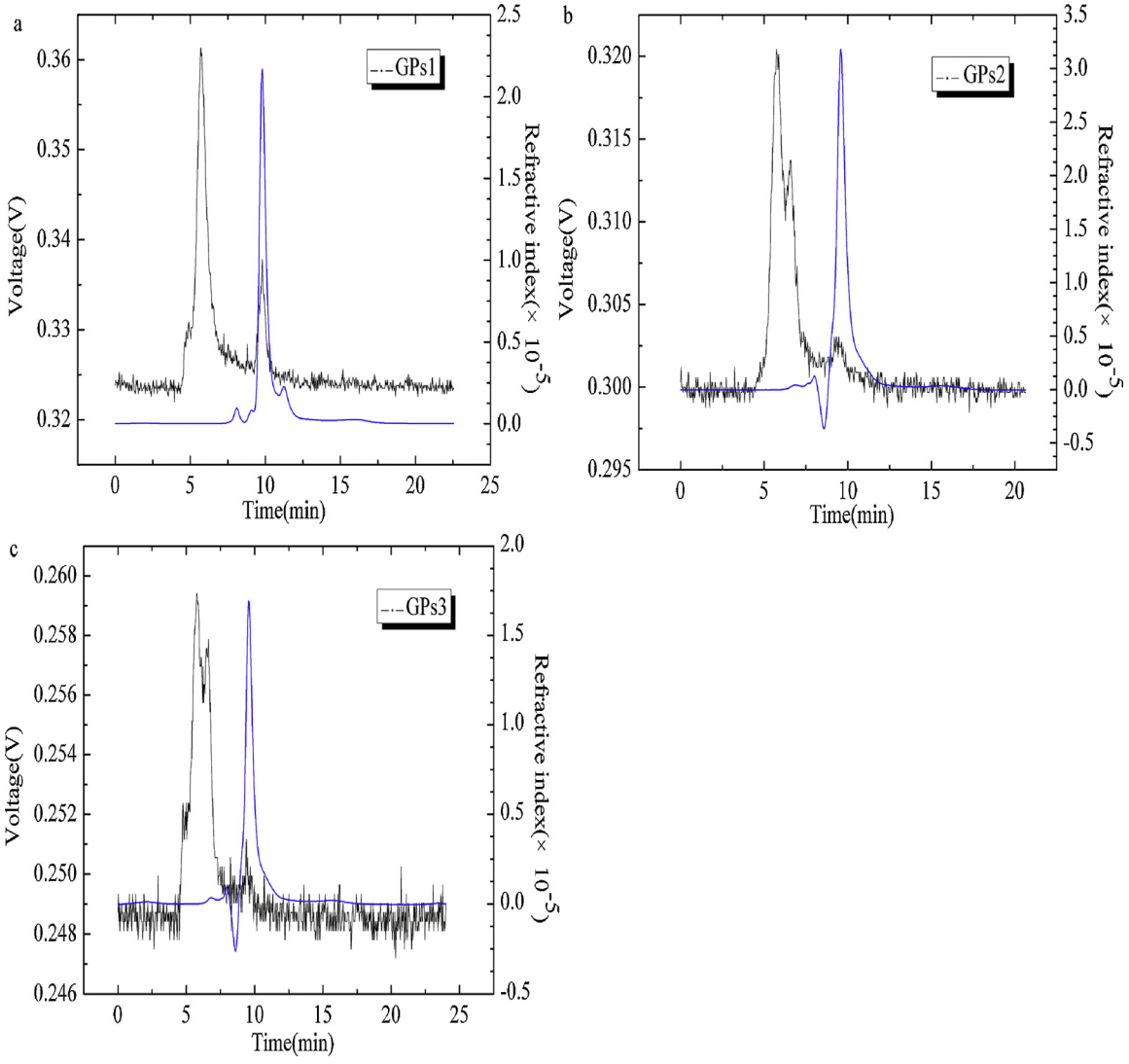

Fig. 4. HPSEC-MALLS chromatograms of GPs1, GPs2 and GPs3.

shown in Table 3, indicating that GPs1, GPs2 and GPs3 exhibited two peaks, three peaks and three peaks, respectively. The Mw of each peak for GPs1 was defined to be 4.513×10^3 g/mol and 8.349×10^2 g/mol, the Mw of each peak for GPs2 was 1.378×10^5 g/mol, 8.559×10^3 g/mol and 2.871×10^2 g/mol, respectively, and the Mw of each peak for GPs3 was defined to be 2.084×10^5 g/mol, 1.092×10^4 g/mol, and 2.606×10^2 g/mol, respectively. The molecular weight distribution of polysaccharide is affected by the mode and factors of polymerization. PD is used as a tool to show the distribution of molecular weight. The molecular weight distribution is wide and the PD value is large. The PD value is closer to 1 and the distribution of the molecular weight is narrower. In Table 3, the value of PD (Mw/Mn) indicated that GPs1 was mainly consisted of the polymers with two different molecular weights, and two components of molar mass of Peak 1 and Peak 2 distribution were inhomogeneous. On the other hand, GPs2 and GPs3 were mainly consisted of the polymers with three different molecular weights, and two components of molar mass of Peak 1 and Peak 3 distribution were more homogeneous than Peak 2. The molecular weigth distribution of also exhibited more difference between the *G. uralensis* of different scourers as shown in Supplementary Table S1. The purified GUPs-1, GUPs-2 and GUPs-3 of polysaccharides from Yanchi, Xining, China were 10 160, 11 680 and 13 360 Da, receptively (Zhang et al., 2015), which was significantly different due to the different extraction technology and material scources. Meanwhile, five kinds of purified polysaccharides from Shihezi, Xinjiang, China were obtained, but not be determined for the molecular weight analysis (Chen et al., 2017).

3.4. Monosaccharide composition and FT-IR spectroscopy

GC–MS analysis of monosaccharide composition of GPs1, GPs2 and GPs3 (Table 4) showed that GPs chromatographic component was relatively simple. GPs1, GPs2 and GPs3 contained glucose and galactose. In addition, GPs2 and GPs3 also contained arabinose. These results were the same as Sun and Zhang (2006) who confirmed that GPs was consisted of glucose, arabinose and galactose, and maybe glucose or galactose was the main chain. However, Zhang et al. reported the three purified fractions of crude *G. uralensis* polysaccharides from Yanchi, Ningxia, China were made up of glucose, galactose, arabinose, rhamnose and mannose (Zhang et al., 2015). And the similar monosaccharide compositions of *G. uralensis* polysaccharides from Shihezi, Xinjiang, China were reported by Chen et al. (2017) as shown in Supplementary Table S1, in which the differences were due to distinct varieties and distributions.

In order to elucidate the structures of GPs1, GPs2 and GPs3, FT-IR were performed and the results were presented in Fig. 5. The fractions in GC chromatogram showed that: a broadly-stretched intense peak at 3600-3200 cm^{-1} characteristic of hydroxyl groups (Ge et al., 2009); a broad band at 3440 cm^{-1} is due to the stretching vibration of hydroxyl group; a weak C—H band at around 2390 cm^{-1}; the relatively strong absorption peak at around 1600-1650 cm^{-1} indicated the characteristic of C═O (Jia et al., 2014), meanwhile, the existence of C═O indicates polysaccharides contain amide bond or carboxylic acid. The absorption band from 1300 cm^{-1} to 800 cm^{-1}, called “finger print” region, is related to conformation and surface structure of molecule. In addition, the region ranging from 950 cm^{-1} to 1200 cm^{-1} suggests the presence of C—O—C, C—O—H link bonds and hydroxyl of pyranose ring, and it demonstrates the presence of pyranose (Jing et al., 2016; Wang et al., 2015); GPs1, GPs2 and GPs3 have these characteristic link bands of polysaccharides. Of course, there were little differences among the spectra of three fractions. A peak at 881 cm^{-1} showed that GPs3 has a β-glycosidic bond, and peaks at 696 cm^{-1} or 648 cm^{-1} may be the characteristic peak of rhamnose (Wei et al., 2017). The FT-IR results were consisted with the physicochemical property of GPs1, GPs2 and GPs3.

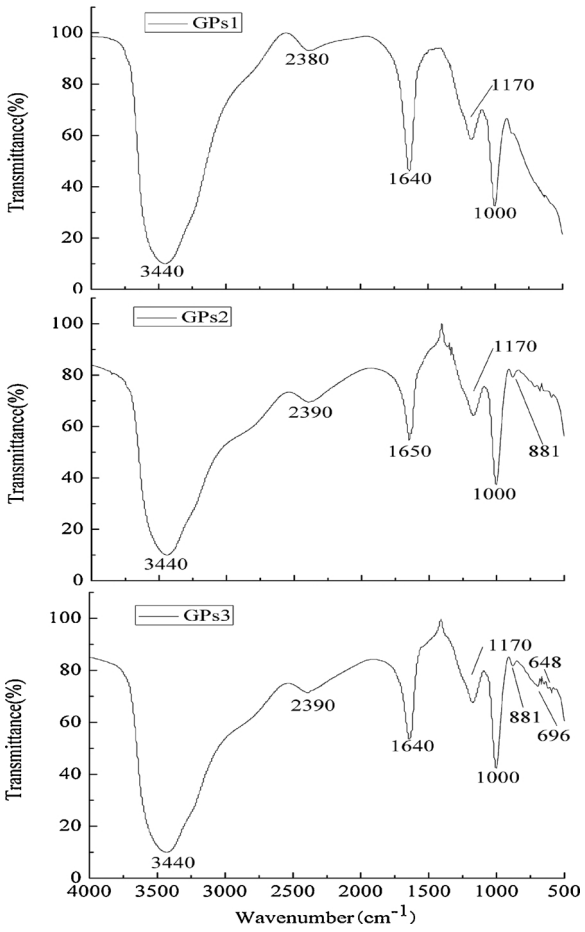

Fig. 5. Infrared absorption spectra of GPs1, GPs2 and GPs3.

Table 4
Monosaccharide compositions of the polysaccharide fractions (GPs1, GPs2 and GPs3) from *G. uralensis*.

Sample	Area (%)					
	Rha	Ara	Xyl	Man	Glu	Gal
GPs1	Nd	Nd	Nd	Nd	56.08	23.97
GPs2	Nd	16.6	Nd	Nd	66.42	19.12
GPs3	Nd	0.48	Nd	Nd	48.88	19.89

Note: The data are presented as mole ratios for each sugar. Individual components were identified and quantified based on elution of known standards. Nd, not detected.

3.5. SEM observation

The structures of GPs1, GPs2 and GPs3 were studied by SEM (Fig. 6). As shown in Fig. 6a, GPs1 was flaky with a pore structure. GPs2 was flaky or clastic with a rough surface and a pore structure (Fig. 6b). While, the structure of GPs3 was different from GPs1 and GPs2, which was irregular with a rough surface and a pore structure (Fig. 6c). Pore structure shows that intermolecular repulsion is existed polysaccharide molecules (Jun et al., 2010), and a pore structure from large to small could be listed as follows: GPs2, GPs1 and GPs3, which was opposite with Qi et al. (2012) who discovered *lycium barbarum* polysaccharide (LBP3-I) has a high branch structure and sugar chains tangled together into rings. Even if magnification didn’t obtain the microscopic morphology information of polysaccharide aggregates, the structure of polysaccharides need to be further analyzed.

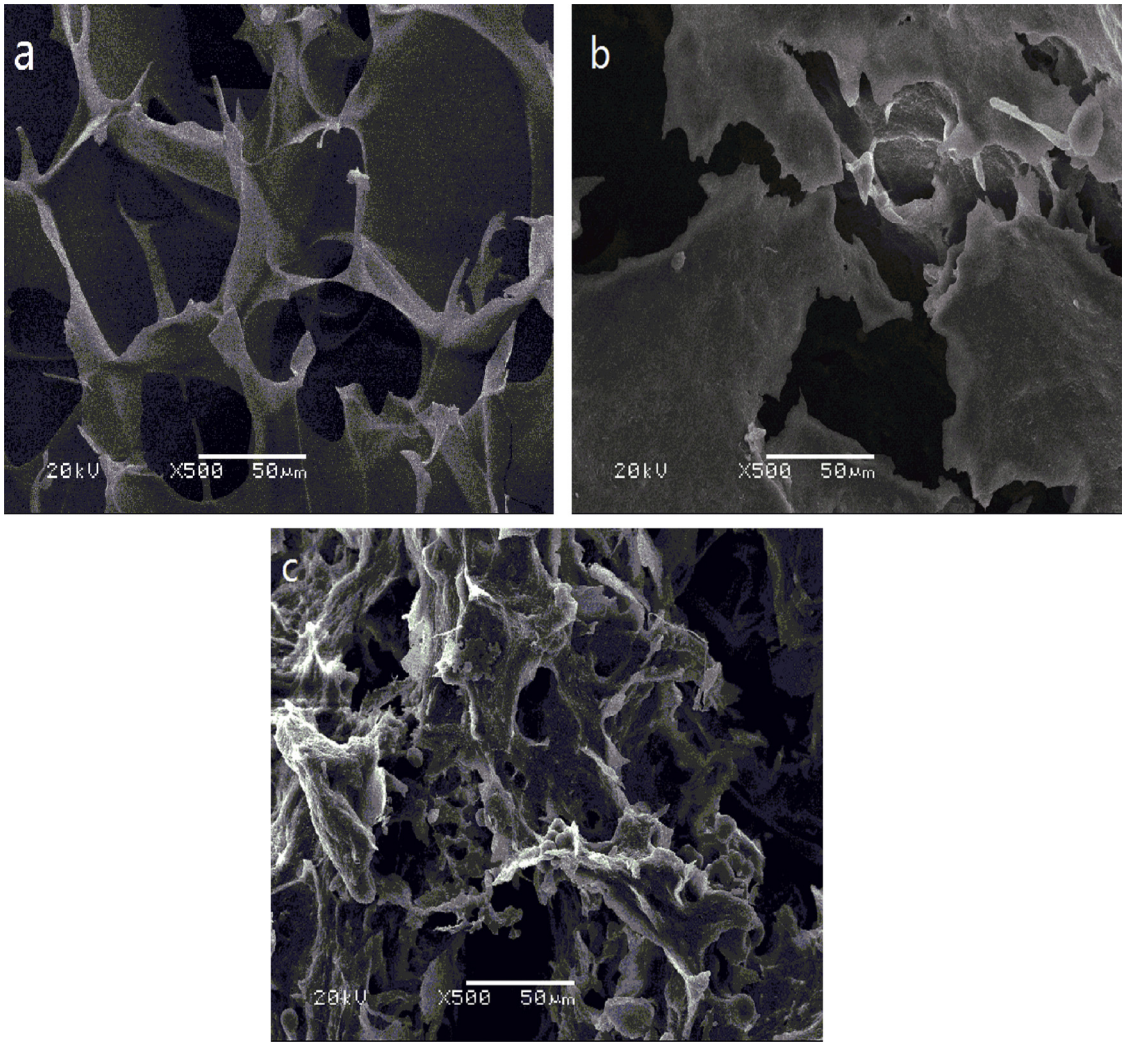

Fig. 6. The microscopic structure of GPs1, GPs2 and GPs3 by SEM (20 KV, ×500, 50 μm).

3.6. AFM observation

Atomic force microscopy (AFM) is a novel material structure analysis method developed on the basis of scanning tunneling microscope. AFM allows the biological macromolecule sample directly to observe under close physiological condition. AFM can provide tridimensional information of biological macromolecules in nano/submicron, and it is suitable for the study of visualization and function of biological macromolecules. Therefore, it has been widely used to study the surface morphology or structure of biomacromolecules. AFM has also been applied successfully on imaging of polysaccharides (Wei et al., 2016).

The molecular morphology of GPs1, GPs2 and GPs3 were depicted in detail by AFM (Fig. 7). Fig. 7a, c, and e depicted the molecular morphology (scanned at 10 × 10 μm) of them, respectively. Fig. 7a and c showed that GPs1 and GPs2 were closely arranged and varied in size. There were a large number of dispersions and a small amount of smaller globular aggregates. While Fig. 7e showed that GPs3 was contrary to the result above mentioned, indicating GPs3 has a greater viscosity of the solution than GPs1 and GPs2. Unlike the Oat β-glucan reported by Wu et al. (2006), of which the spherical aggregates were dispersed into discrete and extended polymer chains with SDS, three purified polysaccharides (GPs1, GPs2 and GPs3) appeared still as spherical chains after dispersion with SDS.

Fig. 7b, d and f showed a tridimensional structure of GPs1, GPs2 and GPs3, respectively, which represented that the height of the aggregation of three purified fractions in the solution. Surface topography of them are rugged and likely composed of many high sharp ends and many irregular protrusions. It also suggested that the structure units of GPs1, GPs2 and GPs3 might be branched and entangled with each other. The results were the same as Li et al. (2017). These directly confirmed that the chemical structure of polysaccharides with highly branched molecules.

3.7. Determination of bioactivities in vitro of GPs

3.7.1. Hydroxyl radical scavenging assay

Hydroxyl radical is an extremely reactive chemical species which can react with any biological molecule and their damaging action is the strongest among free radical species (Jiang et al., 2010). Hydroxyl radical (OH^-) can easily cross cell membranes and react readily with most biomolecules including carbohydrates, proteins, lipids, and DNA in cells to cause tissue damage even cell death (Yuan et al., 2012). Removing HO^- and superoxide radical is important for the protection of living systems. Hydroxyl radicals were generated in an H_2O_2-$FeSO_4$ system and assayed by the oxidation of salicylic acid. The results in Fig. 8a showed hydroxyl radical scavenging assay of GPs0, GPs1, GPs2 and GPs3 at different concentrations with ascorbic acid (Vc) as the positive control. The hydroxyl radical scavenging activities were enhanced with increased concentration. HO^- scavenging activity of Vc was the highest. The highest scavenging activity was 83.10% for Vc (2.5 mg/mL) while those of the remainder of GPs from large to small could be listed as follows: GPs1, GPs0, GPs2, and GPs3.

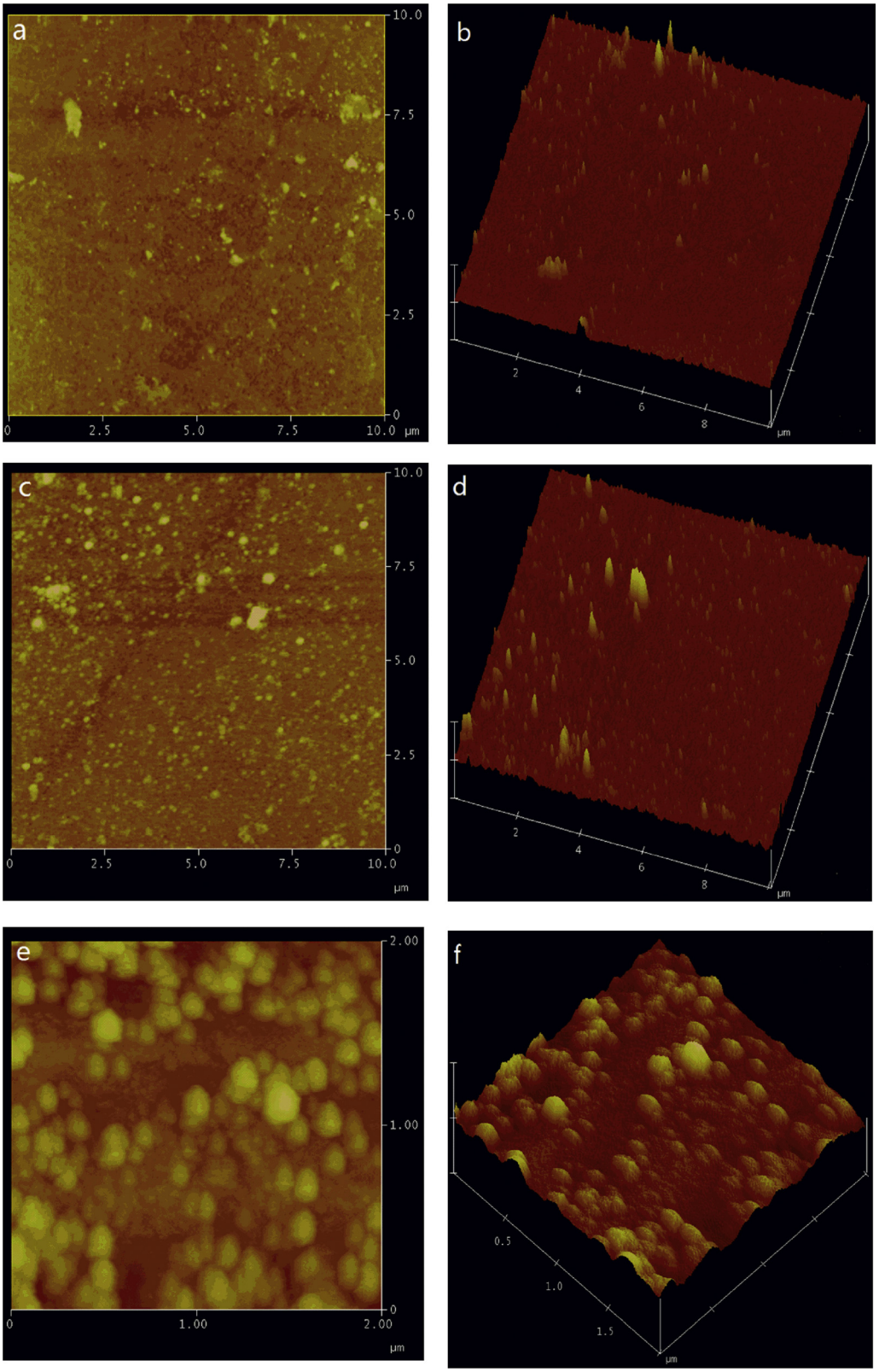

Fig. 7. The microscopic molecular morphology of GPs1, GPs2 and GPs3 by AFM (a, b, c, d: Scan size 10 μm; e, f: Scan size 2.0 μm).

3.7.2. Superoxide radical scavenging assay

Superoxide radical is a highly toxic species generated by numerous biological and photochemical reactions (Banerjee et al., 2005). The scavenging superoxide radical effects of GPs0, GPs1, GPs2, GPs3 and Vc were shown in Fig. 8b. The highest superoxide radical scavenging ratio (64.25%) of GPs was achieved at the concentration of 4.0 mg/mL, which was lower compared with that of ascorbic acid (93.67%). As expected, all the GPs samples in this study possess superoxide radical scavenging activities, especially GPs1 shown relatively the strongest activities. The scavenging effects of the specimens on superoxide

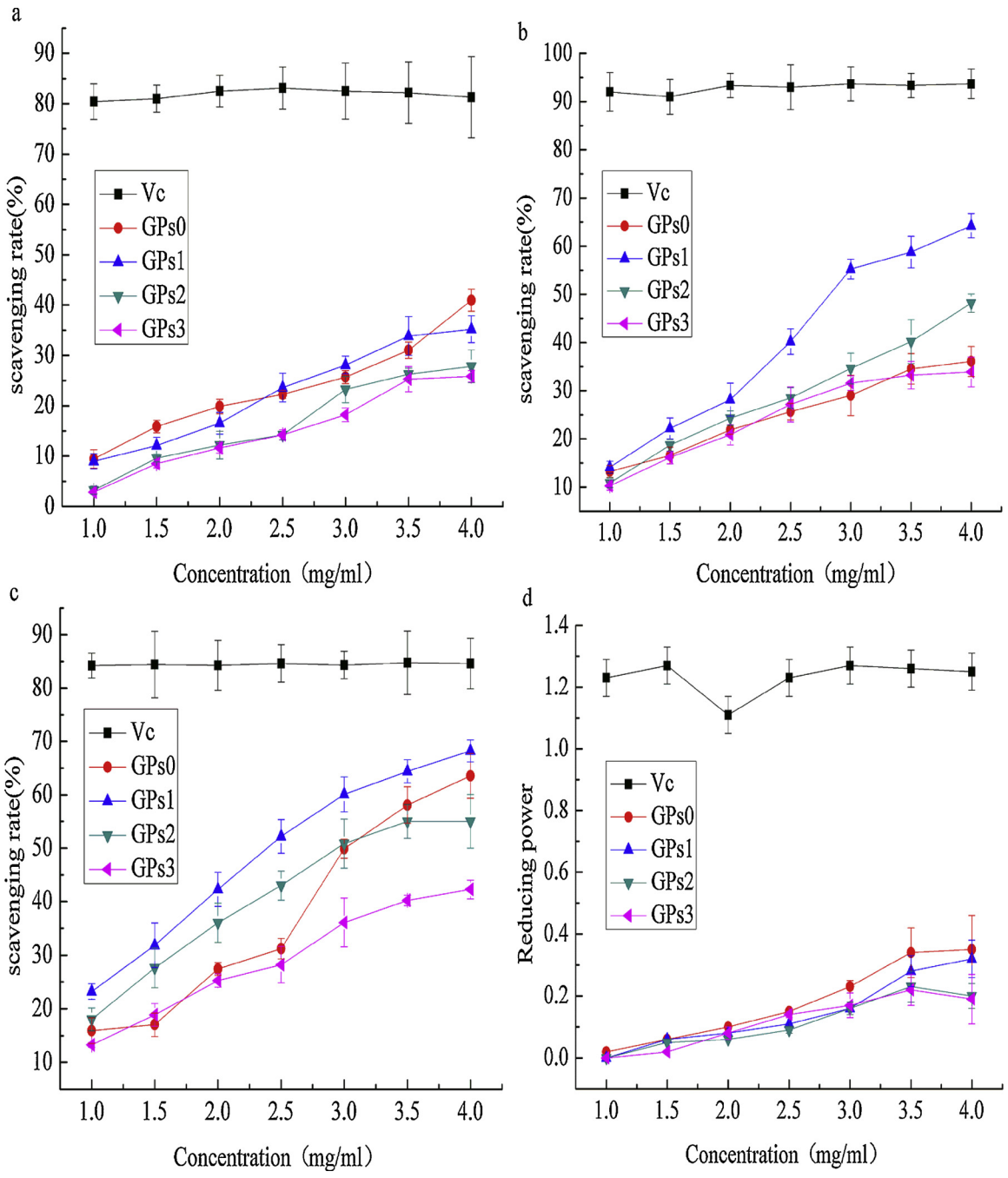

Fig. 8. Antioxidant activities of GPs0, GPs1, GPs2, GPs3 and Vc: a. Scavenging activity of hydroxyl radical; b. Scavenging ability of superoxide anion; c. Scavenging ability of DPPH radicals; d. Reducing power. Data were shown as mean (n = 3). The vertical bars represented the standard deviation of each data point ($P < 0.05$).

radical was in the order of large to small: Vc, GPs1, GPs2, GPs0, and GPs3 within the experimental concentration in the range of 1.0–4.0 mg/mL. These results indicated that GPs1 really has a good scavenging activity of superoxide radicals, and it might be helpful to prevent the damage induced by superoxide radicals under pathological conditions (Zhang et al., 2015).

3.7.3. DPPH radicals scavenging assay

The model of scavenging the stable DPPH radical is a widely used method to evaluate the free radical scavenging ability of natural compounds and the DPPH free radicals are stable and commercially available organic nitrogen radicals which can accept an electron or hydrogen radical to become a stable molecule (Chen et al., 2008). An alcoholic solution of DPPH has a UV–vis absorption maximum at 517 nm (Li and Shah, 2014; Raza et al., 2017). The scavenging activity of GPs and Vc on the DPPH radicals were shown in Fig. 8c. The highest scavenging ratio of DPPH radicals of GPs1 (68.23%) was observed at 4.0 mg/mL, which was weaker than that of ascorbic acid (84.63%). The results indicated that the ability of GPs1 to transfer electrons or hydrogen atoms was stronger than that of GPs0, GPs2 and GPs3. From the figure, the scavenging ability of GPs1 on DPPH radicals was concentration dependent, which was consistent with Chen et al. (2017) and Zhang et al. (2015).

3.7.4. Total reduce power assay

The reducing power of a compound may serve as a significant indicator of its potential antioxidant activity. A relationship between the reduce power of bioactive compounds and their antioxidant activity can

be listed as follows: stronger reduce power has higher antioxidant activity. The value of each sample reaction after the resultant light absorption at 700 nm reflects its antioxidant activity. The value of absorption is larger and its antioxidant activity is higher. The determination of reducing powers of GPs0, GPs1, GPs2, GPs3 and Vc were shown in Fig. 8d. The reducing power of Vc was significantly higher than that of GPs. GPs0 exhibited stronger reducing power than GPs1, GPs2 and GPs3, but within the concentration ranging from 1.0 to 4.0 mg/mL, all of the GPs exhibited lower activity than Vc. The reducing property is generally associated with the capacity of reacting with certain precursors of peroxide and preventing peroxide formation (Song et al., 2015; Raza et al., 2017). Based on this theory, compared with GPs1, GPs2 and GPs3, GPs0 may have a better ability to donate electrons and reduce peroxide.

4. Conclusion

The extraction conditions of polysaccharide were optimized based on RSM. Polysaccharide was separated and purified from *G. uralensis* through DEAE-52 and Sephadex G-100 column chromatography. The yield of GPs0 reached at the maximum of 4.23%, when the optimum extraction process was 1:13 g/mL (solid-liquid ratio), 600 W (ultrasonic power) at 70 °C for 85 min. Except for GPs2, the others (GPs0, GPs1 and GPs3) are non-reducing sugars. They don't contain starch. GPs0 and GPs1 contain protein. The molecular weight, monosaccharide composition and FT-IR spectroscopy assay showed that GPs1, GPs2 and GPs3 are pyran polysaccharides with a weight average molecular weight (Mw) of 4.513×10^3, 1.378×10^5 and 2.084×10^5 g/mol, respectively. GPs1, GPs2 and GPs3 mainly contain glucose and galactose, respectively. SEM observation showed that GPs1, GPs2 and GPs3 are flaky with a pore structure. AFM observation revealed GPs1 and GPs2 molecules both have a large number of dispersions and a small amount of smaller globular aggregates. GPs3 is contrary to the result above mentioned. The antioxidant activity assay of three purified polysaccharides illustrated that GPs1 has the strongest scavenging effect within the test objects. Therefore, it was confirmed that GPs1 would have wide application in the biomedical engineering and food science. Further *in vivo* experiments on biological activities of polysaccharides are in progress, and we are trying to clarify the antioxidatant mechanism.

Acknowledgement

This research was supported by National Natural Science Foundation of China (Nos. 31460032, 81660581).

References

Aguiló-Aguayo, I., Walton, J., Viñas, I., Tiwari, B.K., 2017. Ultrasound assisted extraction of polysaccharides from mushroom by products. LWT-Food Sci. Technol. 77, 92–99.
Banerjee, A., Dasgupta, N., De, B., 2005. *In vitro* study of antioxidant activity of *Syzygium cumini* fruit. Food Chem. 90 (4), 727–733.
Bitter, T., Muir, H.M., 1962. A modified uronic acid carbazole reaction. Anal. Biochem. 4 (4), 330–334.
Chen, Y., Xie, M.Y., Nie, S.P., Li, C., Wang, Y.X., 2008. Purification, composition analysis and antioxidant activity of a polysaccharide from the fruiting bodies of Ganoderma atrum. Food Chem. 107 (1), 231–241.
Chen, J., Zhu, X.Q., Yang, L., Luo, Y., Wang, M.Y., Liu, X.T., Liang, K.X., Gu, X.L., 2016. Effect of *Glycyrrhiza uralensis* Fisch polysaccharide on growth performance and immunologic function in mice in Ural City, Xinjiang. Asian Pac. J. Trop. Med. 9 (11), 1078–1083.
Chen, J., Li, W., Gu, X., 2017. Optimized extraction, preliminary characterization, and *in vitro* antioxidant activity of polysaccharides from *glycyrrhiza uralensis* fisch. Med. Sci. Monit. 23, 1783–1791.
Cheng, A., Wan, F., Jin, Z., Wang, J., Xu, X., 2008. Nitrite oxide and inducible nitric oxide synthase were regulated by polysaccharides isolated from *glycyrrhiza uralensis* fisch. J. Ethnopharmacol. 118 (1), 59–64.
Chihara, G., Maeda, Y., Hamuro, J., Sasaki, T., Fukuoka, F., 1969. Inhibition of mouse sarcoma 180 by polysaccharides from *lentinus edodes* (berk.) sing. Nature 222 (5194), 687–688.
Deng, P., Zhang, G., Zhou, B., Lin, R., Jia, L., Fan, K., Liu, X., Wang, G., Wang, L., Zhang, J., 2011. Extraction and *in vitro* antioxidant activity of intracellular polysaccharide by *pholiota adiposa* SX-02. J. Biosci. Bioeng. 111 (1), 50–54.
Dubois, M., Gilles, K.A., Hamilton, J.K., Rebers, P.A., Smith, Fred, 1956. Colorimetric method for determination of sugars and related substances. Anal. Chem. 28 (3), 350–356.
Feng, K., Chen, W., Sun, L., Liu, J., Zhao, Y., Li, L., Wang, Y., Zhang, W., 2015. Optimization extraction, preliminary characterization and antioxidant activity *in vitro* of polysaccharides from Stachys sieboldii miq. tubers. Carbohyd. Polym. 125, 45–52.
Ge, Y., Duan, Y., Fang, G., Zhang, Y., Wang, S., 2009. Polysaccharides from fruit calyx of *Physalis alkekengi* var. francheti: isolation, purification, structural features and antioxidant activities. Carbohyd. Polym. 77 (2), 188–193.
Ghasemzadeh, A., Jaafar, H.Z.E., Rahmat, A., 2015. Optimization protocol for the extraction of 6-gingerol and 6-shogaol from *zingiber officinale* var. *rubrum theilade* and improving antioxidant and anticancer activity using response surface methodology. BMC Complem. Altern. M. 15 (1), 258.
Huang, X.L., Wu, H.Q., Huang, F., Lin, X.S., 2006. Analysis of polysaccharide from broken cellular wall and unbroken spore of Ganoderma lucidum. Chin. Tradit. Herb. Drugs 37 (6), 813–816 (in Chinese).
Ji, X., Peng, Q., Yuan, Y., Liu, F., Wang, M., 2017. Extraction and physicochemical properties of polysaccharides from *ziziphus jujuba* cv. muzao by ultrasound-assisted aqueous two-phase extraction. Int. J. Biol. Macromol. 108, 541–549.
Jia, X., Ding, C., Yuan, S., Zhang, Z., Chen, Y., Du, L., Yuan, M., 2014. Extraction, purification and characterization of polysaccharides from hawk tea. Carbohyd. Polym. 99 (1), 319–324.
Jiang, Y.H., Jiang, X.L., Wang, P., Hu, X.K., 2010. In vitro *In vitro* antioxidant activities of water-soluble polysaccharides extracted from *Isaria farinosa* B05. J. Food Biochem. 29 (3), 323–335.
Jiang, J., Kong, F., Li, N., Zhang, D., Yan, C., Lv, H., 2016. Purification, structural characterization and *in vitro* antioxidant activity of a novel polysaccharide from *boshuzhi*. Carbohyd. Polym. 147, 365–371.
Jin, M., Cai, Y.X., Li, J.R., Zhao, H., 1996. 1, 10-Phenanthroline-Fe^{2+} oxidative assay of hydroxyl radical produced by H_2O_2/Fe^{2+}. Prog. Biochem. Biophys 23 (6), 553–555.
Jing, F., Feng, H., Yu, Y., Sun, M., Liu, Y., Li, T., Xin, S., Liu, S., Sun, M., 2016. Antioxidant activities of the polysaccharides of Chuanminshen violaceum. Carbohyd. Polym. 157, 629–636.
Jun, L.I., Zhong, Y.G., Liu, C.J., 2010. Purification and electron microscope analysis of lentinan. J. Shanxi Agric. Sci. 38 (3), 6–9 (in Chinese).
Kawai, Y., Seno, N., Anno, K., 1969. A modified method for chondrosulfatase assay. Anal. Biochem. 32 (2), 314–321.
Lee, J.W., Xiao, N.Q., Yu, R.Y., Yuan, M.X., Chen, L.R., Chen, Y.H., Chen, L.T., 1994. Principles and Methods of Biochemistry Experiment. Beijing University Press, Beijing, pp. 151–278 . (in Chinese).
Li, S., Shah, N.P., 2014. Antioxidant and antibacterial activities of sulphated polysaccharides from pleurotus eryngii and *Streptococcus thermophilus* ASCC 1275. Food Chem. 165, 262–270.
Li, X., Wang, L., Wang, Z., 2017. Structural characterization and antioxidant activity of polysaccharide from *Hohenbuehelia serotina*. Int. J. Biol. Macromol. 98, 59–66.
Ma, T., Sun, X., Tian, C., Luo, J., Zheng, C., Zhan, J., 2016. Polysaccharide extraction from sphallerocarpus gracilis roots by response surface methodology. Int. J. Biol. Macromol. 88, 162–170.
Maclennan, C.A., Richter, A., Hodson, J., Faustini, S., Birtwistle, J., Whitelegg, A., Chigiga, J., Singo, M., Walker-Haywood, J., Mulugeta, B., 2016. Immunization of hiv-infected adults in the UK with haemophilus influenzae b/meningococcal C glycoconjugate and pneumococcal polysaccharide vaccines. J. Acquir. Immune Defic. Syndr. 73 (3), 287–293.
Patel, A.K., Laroche, C., Marcati, A., Ursu, A.V., Jubeau, S., Marchal, L., Petit, E., Djelveh, G., Michaud, P., 2013. Separation and fractionation of exopolysaccharides from porphyridium cruentum. Bioresour. Technol. 145 (5), 345–350.
Prabhjit, K., Neha, S., Bikram, S., Subodh, K., Satwinderjeet, K., 2012. Modulation of genotoxicity of oxidative mutagens by *glycyrrhizic* acid from *glycyrrhiza glabral*. Pharmacogn. Res. 4 (4), 189–195.
Prakash, M.J., Sivakumar, V., Thirugnanasambandham, K., Sridhar, R., 2013. Optimization of microwave assisted extraction of pectin from orange peel. Carbohyd. Polym. 97 (2), 703–709.
Qazvini, N.T., Zinatloo, S., 2011. Synthesis and characterization of gelatin nanoparticles using CDI/NHS as a non-toxic cross-linking system. J. Mater. Sci. Mater. Med. 22 (1), 63–69.
Qi, G., Sun, R.G., Guo, G.Y., 2012. Isolation and purification, its structure spectral analysis, and microscopy observation of *Lycium barbarum* polysaccharide. Chin. Tradit. Herb. Drugs 43 (4), 645–648 (in Chinese).
Raza, A., Li, F., Xu, X., Tang, J., 2017. Optimization of ultrasonic-assisted extraction of antioxidant polysaccharides from the stem of Trapa quadrispinosa using response surface methodology. Int. J. Biol. Macromol. 94 (Pt A), 335–344.
Ren, B., Chen, C., Li, C., Fu, X., You, L., Liu, R.H., 2017. Optimization of microwave-assisted extraction of *Sargassum thunbergii* polysaccharides and its antioxidant and hypoglycemic activities. Carbohyd. Polym. 173, 192–201.
Romdhane, M.B., Haddar, A., Ghazala, I., Jeddou, K.B., Helbert, C.B., Ellouz-Chaabouni, S., 2017. Optimization of polysaccharides extraction from watermelon rinds: structure, functional and biological activities. Food Chem. 216, 355–364.
Rui, J., Liu, Y., Hao, G., Jia, X., So, K.F., 2016. The anti-oxidant and antitumor properties of plant polysaccharides. Am. J. Chin. Med. 44 (3), 463–488.
Sarin, V.K., Kent, S.B., Tam, J.P., Merrifield, R.B., 1981. Quantitative monitoring of solid-phase peptide synthesis by the ninhydrin reaction. Anal. Biochem. 117 (1), 147–157.
Schneider, F., 1979. Sugar Analysis: Official and Tentative Methods Recommended by the International Commission for Uniform Methods of Sugar Analysis. ICUMSA, Peterborough, pp. 41–73.

Shen, S., Chen, D., Li, X., Li, T., Yuan, M., Zhou, Y., Ding, C., 2014. Optimization of extraction process and antioxidant activity of polysaccharides from leaves of Paris polyphylla. Carbohyd. Polym. 104 (104), 80–86.
Shimada, K., Fujikawa, K., Yahara, K., Nakamura, T., 1992. Antioxidative properties of xanthan on the autoxidation of soybean oil in cycloextrin emulsion. J. Agric. Food Chem. 40 (6), 945–948.
Song, Y., Ni, Y., Hu, X., Li, Q., 2015. Effect of phosphorylation on antioxidant activities of pumpkin (Cucurbita pepo, Lady godiva) polysaccharide. Int. J. Biol. Macromol. 81, 41–48.
Sun, R.G., Zhang, J., 2006. A study of helical structure of *glycyrrhiza* polysaccharides by atomic force microscope. Acta Chim. Sin. 64 (24), 2467–2472.
Wang, J., Zhang, J., Zhao, B., Wang, X., Wu, Y., Yao, J., 2010. A comparison study on microwave-assisted extraction of *Potentilla anserina* L. polysaccharides with conventional method: molecule weight and antioxidant activities evaluation. Carbohyd. Polym. 80 (1), 84–93.
Wang, Y., Wang, F., Ma, X., Sun, S., Leng, F., Zhang, W., Wang, X., 2015. Extraction, purification, characterization and antioxidant activity of polysaccharides from piteguo fruit. Ind. Crop. Prod. 77 (2), 467–475.
Wei, C.Y., Li, W.Q., Shao, S.S., He, L., Cheng, J., Han, S., Liu, Y., 2016. Structure and chain conformation of a neutral intracellular heteropolysaccharide from mycelium of Paecilomyces cicadae. Carbohyd. Polym. 136 (4), 728–737.
Wei, Q., Ren, D.M., Li, S.C., Sun, T., Lv, L.H., 2017. Extraction and purification of polysaccharides from stems and leaves of Taxus grown in Mountain areas in Southern Anhui Province and their monosaccharide composition. Food Sci. 38 (16), 1–10 (in Chinese).
Wu, J., Zhang, Y., Wang, L., Xie, B., Wang, H., Deng, S., 2006. Visualization of single and aggregated *Hulless oat* (Avena nuda L.) (1→3), (1→4)- β-D-glucanmolecules by atomic force microscopy and confocal scanning laser microscopy. J. Agr. Food Chem. 54 (3), 925–934.
Yang, S., Li, Y., Jia, D., Yao, K., Liu, W., 2017. The synergy of box-behnken designs on the optimization of polysaccharide extraction from mulberry leaves. Ind. Crop. Prod. 99, 70–78.
Yi, W., Lei, Y., Li, E., Li, Y., Yan, L., Wang, P., Zhou, H., Liu, J., Hu, Y., Wang, D., 2017. Optimization of *glycyrrhiza* polysaccharide liposome by response surface methodology and its immune activities. Int. J. Biol. Macromol. 102, 68–75.
Ying, Z., Han, X., Li, J., 2011. Ultrasound-assisted extraction of polysaccharides from mulberry leaves. Food Chem. 127 (3), 1273–1279.
Yuan, Z.B., Gao, R.M., 1997. Kinetics and mechanism of pyrogallol autoxidation. Chem. Res. Chin. U 18, 1438–1441 (in Chinese).
Yuan, Y., Macquarrie, D., 2015. Microwave assisted extraction of sulfated polysaccharides (Fucoidan) from *Ascophyllum nodosum*, and its antioxidant activity. Carbohyd. Polym. 129, 101–107.
Yuan, J.F., Zhang, Z.Q., Fan, Z.C., Yang, J.X., 2012. Antioxidant effects and cytotoxicity of three purified polysaccharides from Ligusticum chuanxiong hort. Carbohyd. Polym. 74 (4), 822–827.
Zhang, W.J., Wang, P., Wang, Y.G., Fu, W.D., Pu, X.Y., Zhang, F., Hua, D.W., Ma, S.J., Chen, Z., Wang, M.G., 2013. Preparation and characterization of porous Chuanxiong polysaccharide/squid skin collagen composite scaffolds. J. Biobased Mater. Bio. 7 (3), 323–330.
Zhang, C.H., Yu, Y., Liang, Y.Z., Chen, X.Q., 2015. Purification, partial characterization and antioxidant activity of polysaccharides from *Glycyrrhiza uralensis*. Int. J. Biol. Macromol. 79, 681–686.
Zhang, W.J., Chen, Z., Ma, S.J., Wang, Y.G., Zhang, F., Wang, K.Y., Yang, C.G., Pu, X.Y., Ma, J.Z., Wang, Y.L., Leng, F.F., Ran, F., Kuang, Y.B., 2016. Cistanche polysaccharide (CDPS)/polylactic acid (PLA) scaffolds based coaxial electrospinning for vascular tissue engineering. Int. J. Polym. Mater. 65 (1), 38–46.
Zhang, W.J., Zhao, L., Ma, J.Z., Yang, C.G., Wang, X.C., Pu, X.Y., Wang, Y.G., Ran, F., Wang, Y.L., Ma, H., 2017. A kind of injectable angelica sinensis polysaccharide(asp)/hydroxyapatite (hap) material for bone tissue engineering promoting vascularization, hematopoiesis, and osteogenesis in mice. Int. J. Polym. Mater. 67 (4), 205–211.
Zinatloo, S., Qazvini, N.T., 2014. Inverse miniemulsion method for synthesis of gelatin nanoparticles in presence of CDI/NHS as a non-toxic cross-linking system. J. Nanostruct. 4 (3), 267–275.
Zinatloo, S., Qazvini, N.T., 2015. Effect of some synthetic parameters on size and polydispersity index of gelatin nanoparticles cross-linked by CDI/NHS system. J. Nanostruct. 5 (2), 137–144.
Zinatlooajabshir, S., Salehi, Zahra, Salavatiniasari, M., 2016a. Preparation, characterization and photocatalytic properties of $Pr_2Ce_2O_7$ nanostructures via a facile way. RSC Adv. 6 (109), 1–8.
Zinatlooajabshir, S., Mortazaviderazkola, S., Salavatiniasari, M., 2018a. Nd_2O_3-SiO_2 nanocomposites: a simple sonochemical preparation, characterization and photocatalytic activity. Ultrason. Sonochem. 42, 171–182.
Zinatloo-Ajabshir, S., Salavati-Niasari, M., 2015. Novel poly(ethyleneglycol)-assisted synthesis of praseodymium oxide nanostructures via a facile precipitation route. Ceram. Int. 41 (1), 567–575.
Zinatloo-Ajabshir, S., Salavati-Niasari, M., 2016a. Zirconia nanostructures: novel facile surfactant-free preparation and characterization. Int. J. Appl. Ceram. Technol. 13 (1), 108–115.
Zinatloo-Ajabshir, S., Salavati-Niasari, M., 2017. Facile synthesis of nanocrystalline neodymium zirconate for highly efficient photodegradation of organic dyes. J. Mol. Liq. 243, 219–226.
Zinatloo-Ajabshir, S., Salavati-Niasari, M., 2016b. Zirconia nanostructures: novel facile surfactant-free preparation and characterization. Int. J. Appl. Ceram. Technol. 13 (1), 108–115.
Zinatloo-Ajabshir, S., Mortazaviderazkola, S., Salavatiniasari, M., 2018b. Nd_2O_3-SiO_2 nanocomposites: a simple sonochemical preparation, characterization and photocatalytic activity. Ultrason. Sonochem. 42, 171–182.
Zinatloo-Ajabshir, S., Salehi, Zahra, Salavatiniasari, M., 2016b. Preparation, characterization and photocatalytic properties of $Pr_2Ce_2O_7$ nanostructures via a facile way. RSC Adv. 6 (109), 1–8.